Available online at www.sciencedirect.com
SCIENCE DIRECT®
Thermochimica Acta 432 (2005) 192–201
thermochimica acta
www.elsevier.com/locate/tca

Overview of calorimeter chips for various applications

A.W. van Herwaarden*

Xensor Integration, Distributieweg 28, 2645 EJ Delfgauw, The Netherlands

Abstract

This paper gives an overview of some of the recent developments in the area of chip calorimetry. Using several chip calorimeters developed at Xensor Integration and tested by users, examples of chip calorimetry and its applications will be given. Examples of chip calorimeters developed at various universities are given to widen the overview. The examples will be used to give more insight in the design and fabrication of various chip calorimeters.

Keywords: Chip calorimeter; Micro calorimeter; Nano calorimeter; High-speed calorimetry

1. Introduction

The science of calorimetry is more than 200 years old. Since then, many calorimetric instruments have been devised and refined. In the last decades, improving technology has been enabling, but also demanding, that calorimetry becomes smaller, faster, more accurate [1]. For the analysis of very thin films and particles, measured in micrometers and even nanometers, weighed in micrograms or nanograms, even the most refined DSC instruments simply are not adequate anymore. The same holds for the high-speed calorimetric analysis. The speed of production processes is ever increasing to reduce costs. The speed of calorimetric analysis has to keep up, and where DSC rate of heating and cooling is measured in K/min, some applications really require speeds expressed in kK/s.

The silicon technology used to make computer chips also makes it possible to make different chips, which will actually work as calorimeters, measuring nanogram samples at speeds up to 1 MK/s. The secret is to make everything small, especially the heated volumes. This makes it easier to examine minute samples, and to heat and cool at incredible rates.

Chip calorimeters in silicon technology can also be used for chemical analysis in gases and even in liquids. Using different designs, different functions are realized, more appropriate for liquid applications. Here, quite different specifications are attained.

Below, we will give examples of various chip calorimeters developed by Xensor Integration for a number of customers using the chips for a variety of applications. In some cases, these customers have made extensive theoretical studies of the behavior of the chips, and we will refer to these studies. Examples of and references to calorimeter chips of other groups are given as well.

2. Chip calorimeters with mono-crystalline silicon membranes

In 1988 Xensor Integration began with the design of the first closed-membrane chip calorimeters for Ciba-Geigy, who intended to use these devices for measuring the concentration of glucose, penicillin and other substances in a buffered watery solution, and ultimately in blood. In 1990, the first chips (design XI-25) were fabricated, and in the subsequent years Bataillard et al. [2] measured the concentration of glucose, urea and penicillin in the range of 1 mM and 1 M (=mol/l). In order to get very selective sensors, he coated the backside of the membrane with an enzyme, which converts specific substances with a characteristic heat release.

To be able to use his sensors more than once, Bataillard first spin coated the etched cavity of his calorimeter chip with polyvinyl pyridine (from a 2% solution in methanol [2]), and

* Tel.: +31 15 2578040; fax: +31 15 2578050.
E-mail address: svh@xensor.nl.

0040-6031/$ – see front matter © 2005 Published by Elsevier B.V.
doi:10.1016/j.tca.2005.04.027

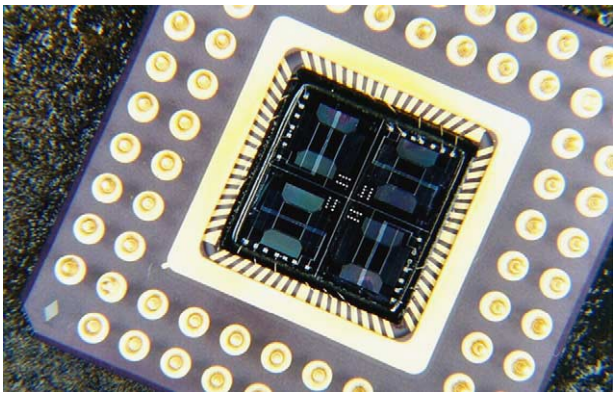

Fig. 1. Four calorimeter chips of type XI-78 mounted in a laser-cut 11 mm × 11 mm hole in a 29 mm × 29 mm ceramic 68-pin PGA.

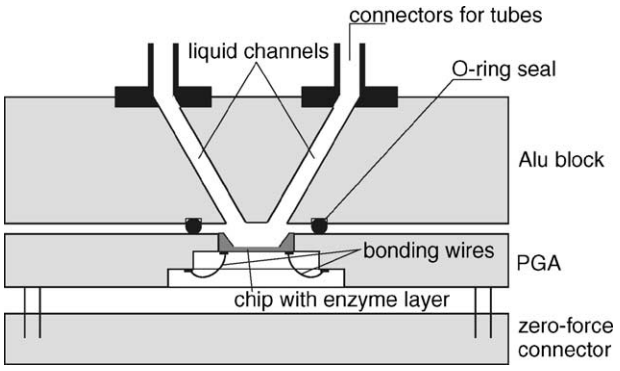

Fig. 3. Heart of the flow injection analysis set-up with the chip calorimeter, zero-force connector and (thermostatted) aluminum block with flow channels [5].

then applied the application-specific enzyme on the polyvinyl pyridine layer. After the enzyme had lost its activity, the layers were removed using methanol.

Most of this work was done with the improved design XI-78, which is a 5 mm × 5 mm chip having a 4 μm thick silicon membrane, see Fig. 1. It is still available today as LCM-2506 and in quad form as LCM-quad [3]. Apart from this, Bataillard also used heavy-duty calorimeter chips of 10 mm × 10 mm with a 22–45 μm thick membrane, Fig. 2, LCM-2524. This chip is no longer made, its successor, NCM-9924 [3] has an aluminum heater added. This makes the electronics design easier, as now no interference can occur between integrated mono-crystalline silicon thermopiles and heaters located in the same epilayer island as in the LCM-2524 (see Fig. 5a).

He also detected the metabolism of living cells immobilized on the calorimeter chip membrane when fed with various concentrations of glucose [4]. For the measurements, Bataillard used a flow-through set-up (Fig. 3), operating the calorimeters in a so-called FIA set-up, flow-injection analysis. In this set-up, buffer liquid is continually flowing past the calorimeter, and every now and then, a sample is injected in this flow, leading to an alternating signal [5]. This also allows eliminating drift of the base line. Fig. 4 shows the measurement of creatinine being alternated with a phosphate buffer solution. This figure clearly shows the return of the base line to zero when the creatinine sample injection is turned off. The sensitivity of this sensor for creatinine was measured to be linear up to 1 M concentration [5].

The alternative to FIA is batch-measurement, in which the sensor is exposed to a batch of non-flowing liquid containing the substance to be analyzed. Then, base line drift cannot be distinguished, but flow irregularities and pressure pulses are absent in this case.

This technique is used by Verhagen at Leuven University, who has also done a lot of work on chip calorimeters for biochemical measurements. Presently she is commercializing a matrix of calorimeters occupying full wafers, containing 96-element titration plate calorimeters for medical and pharmaceutical applications [6]. At 50 nW/3 μJ resolution and 100 nl sample volumes, these calorimeter chips (or actually calorimeter wafers) are truly nanocalorimeters. And at 96

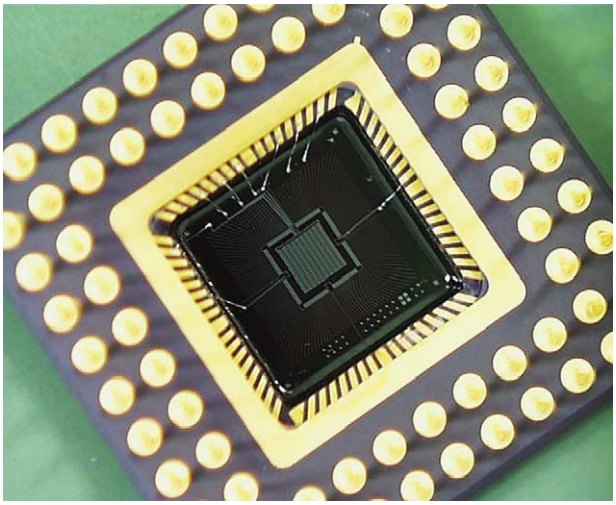

Fig. 2. Heavy-duty calorimeter chip XI-185 mounted in a laser-cut 11 mm × 11 mm hole in a 29 mm × 29 mm ceramic 68-pin PGA.

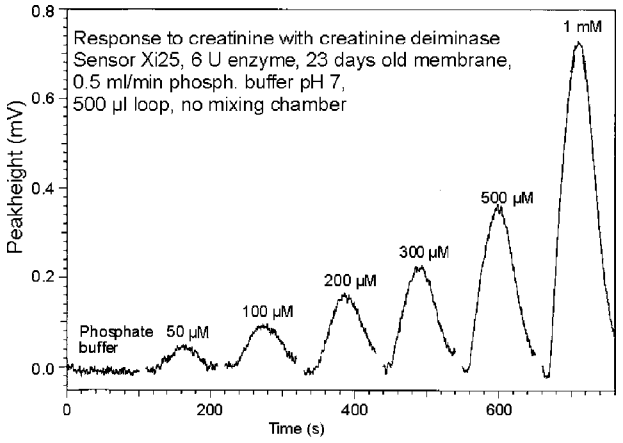

Fig. 4. Response to creatinine of XI-25 liquid calorimeter chip with enzyme layer in FIA set up of Fig. 3 [5].

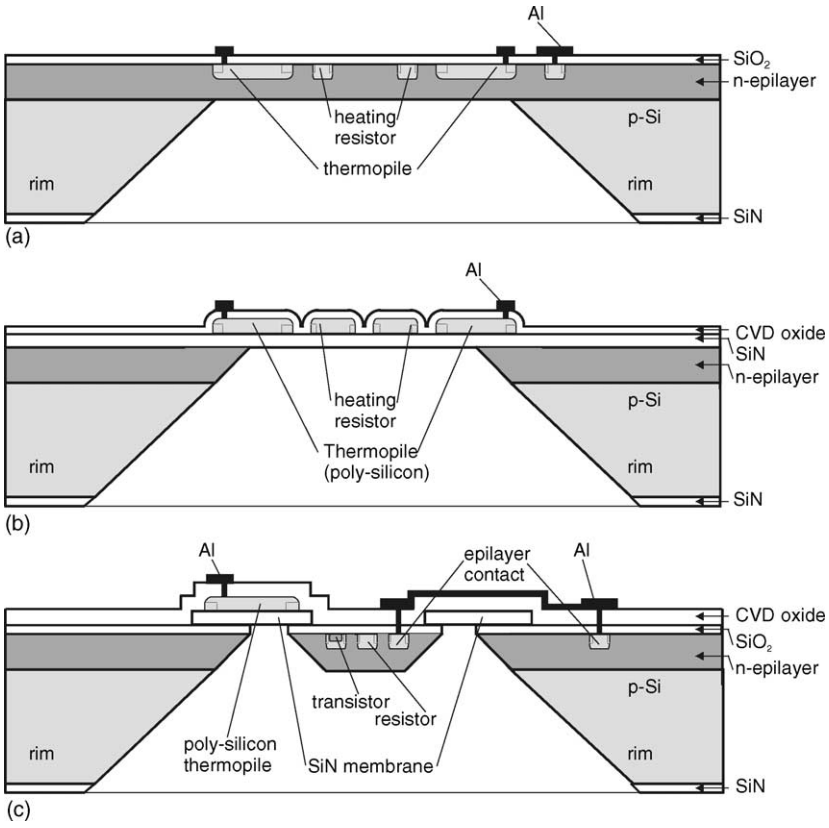

Fig. 5. Some technologies to fabricate chip calorimeters: (a) mono-crystalline Si membrane ($2\frac{1}{2}$–40 μm thick) with mono-Si heating resistors and mono-Si/Al thermopile; (b) SiN membrane with poly-Si heater and thermopile; (c) combined mono-Si/SiN membrane process [7], with poly-Si thermopiles and heaters, and heaters, diodes and transistors in the mono-Si island.

calorimeters analyzing in parallel, the objective of high-speed calorimetry in terms of many analyses per day (100–1000) is also attained.

2.1. Technology

The devices shown above are made with p-type ⟨100⟩ silicon wafers, see Fig. 5a. An n-type epilayer is grown of the desired membrane thickness, i.e. $2\frac{1}{2}$–40 μm thick. In the epilayer, p-type doped strips are created by diffusion or implantation to create heater resistances and the positive legs of a thermopile. The counter legs of the thermopile are then formed by aluminum interconnection, which has a negligible thermoelectric effect. With the typical Seebeck coefficient of p-type mono-silicon of 0.3–0.5 mV/K and 160 thermocouples is series, a thermopile sensitivity of 50–80 mV/K is obtained. Using DSC-type of calibration measurements with the XI-78 (LCM-2506) chip calorimeter, Winter and Höhne found a thermopile sensitivity of about 50 mV/K [8].

Silicon is a very good heat conductor, and a 500 μm thick silicon chip has a negligible thermal resistance in all directions. To increase the thermal resistance and thus the chip calorimeter sensitivity, superfluous silicon is etched away underneath the thermopile, so that only a frame remains as a heat sink and mechanical support for the membrane. This etching is carried out routinely using a 85 °C KOH solution in water (1:2 in weight), and the etching stops at the interface of the p-type substrate and n-type epilayer by electrically biasing the epilayer to at least about 1 V above the etching solution. In this way, the initial thermal resistance of the order of 2 K/W is increased a hundred-fold.

The sensitivity of the chip is thus of the order of 50 mV/K × 200 K/W ≈ 10 V/W. In other words, a heat flow (due to an enzymatically promoted reaction) of 0.1 μW will give 1 μV output signal in air, which will be about the resolution of the calorimeter in a 0.1–1 Hz band width. Winter and Höhne found that in vacuum, the signal might be only a few percent higher [8]. Bataillard found a sensitivity of 8 V/W in air, 3.6 V/W in stationary aqueous solution, and 1.3 V/W in his FIA set-up with a flow of 1 ml/min. This also shows that there is little use in further increasing the thermal resistance of the membrane by making it thinner, if the application is in liquid.

The chip calorimeters of types LCM-2506, LCM-2524 and NCM-9924 have been investigated extensively by Lerchner of the Freiberg Bergakademie for applications in liquids but also in gases, such as the application in an electronic nose [9–14]. Amongst others they measured on small liquid droplets deposited onto the membrane, a kind of mini-batch measurement. In such a set-up evaporation is a major problem, since this will create heat flows of its own. Experiments have further included gas flow-through set-ups (a FIA set-up

with gases instead of liquids) and a scanning-calorimeter set-up. In this latter experiment, the heating rates of 0.5 K/min were not yet so high like those obtained with thin dielectric membranes, as we will see below (kK/s). The low scanning rate is also due to the desire to operate the sensor in an adiabatic manner. Allowing the sensor to have a temperature difference between (the middle of) the membrane and the ambient, operating it in an isoperibolic manner as a conduction sensor allows the much higher scanning rates shown by the dielectric-membrane chip calorimeters.

At Texas University a group is working on liquid calorimeters including reaction chambers. It uses the idea to measure heat of the reaction of two liquids being brought together near the calorimeter, rather than a reaction promoted by an enzyme, which automatically forces the heat to be released at the enzyme layer (=calorimeter chip membrane) [15]. At the Freiberg Bergakademie work is being carried out to implement this idea in a FIA set up such as that of Fig. 3, this requires a second liquid channel towards the liquid volume above the chip, for on-the-spot mixing.

2.2. Figure of merit

Torra et al have been studying the LCM-2524 to establish models to accurately determine the sensitivity of these devices [16–19]. Also these studies concerned measurement in liquid and air, and included calibration comparisons of the on-chip heater with laser-induced local heating, thus creating a 2-D map of the chip calorimeter's local sensitivity.

If the sensitivity of the calorimeter chip as a function of geometry is known, the performance of the device can be judged. Let us define a Figure of Merit $\mathrm{FoM}_{\mathrm{surface}}$ for surface-related calorimeter chips, which will be equal to the output signal of the calorimeter chip, divided by the output noise of the chip. The whole is, of course, normalized to the input signal, which can be, for instance, a concentration in case of a chemical calorimeter, or, for instance, a heat capacity in case of a material properties calorimeter.

For chemical calorimeters detecting surface or volume phenomena, such as calorimeters in liquid with an enzyme layer coverting molecules, the power created will be proportional to the surface area of the membrane. The signal arising from that will be proportional to the effective surface area, since power generated close to the rim of the sensor chip will not create a signal as large as power created in the middle of the membrane. Let us therefore define an effective surface area A^* that takes this effect into account.The output signal will be proportional to A^* for a normalized concentration. The output signal will also be proportional to the transfer S of the chip in, for instance, V/W. This transfer is largely a matter of design, technology and circumstances. For instance, the transfer of even a chip with a thick silicon membrane may decrease almost a factor of 10 when being used in flowing watery liquid instead of air. Nevertheless, these transfer figures are easily known from the chip characterization and can be inserted into the formula. Finally, the noise voltage u_{n} can be inserted into formula to arrive at the following expression for chemical calorimeter chips:

$$\mathrm{FoM}_{\mathrm{surface}} = \frac{A^* S}{u_{\mathrm{n}}} \,\mathrm{in\,m^2 Hz^{1/2}/W} \tag{1}$$

In this example, the FoM does not include the time constant of the device. This expression is not unlike figures of merit found for infrared sensors, which is not surprising because of the close familiarity of the devices. Other figures of merit used for infrared sensors can also be used here, such as noise-equivalent power ($u_{\mathrm{n}}\sqrt{B}/S$) with $\sqrt{B}$ as the square root of the band with in which we measure. For liquid applications a small band width such as 1 Hz is often used.

3. Chip calorimeters with dielectric membranes

3.1. Technology

While a lot of work has been done on chip calorimeters with mono-crystalline silicon membranes, more work has been done on chip calorimeters with dielectric membranes. Here, a membrane based on a low-stress silicon-nitride layer is preferred, because of the excellent mechanical properties of such a layer and its relatively low thermal conductivity. Usually, this silicon-rich SiN layer is best characterized by its refractive index, which is towards 2.2, and a stoichiometric ratio of Si versus N of 0.9 approximately, where 0.75 is the normal ratio. For convenience, this layer is designated as SiN. The technology of such a device is shown in Fig. 5b. The low thermal conductivity of the SiN, together with its smaller thickness, makes that the membrane thermal resistance between the middle and the silicon frame is now routinely of the order of 5–50 kK/W in vacuum, compared to a few hundred K/W for the mono-Si closed membranes. This enables us to detect much smaller heat effects.

However, in order not to spoil the high thermal resistance, thermopiles are usually less sensitive in these devices at 1–5 mV/K. So, the overall sensitivity in air is then of the order of 10–100 V/W, about one order of magnitude higher than for silicon-membrane chips.

Xensor Integrated fabricated in 1991 the thin-film design XI-50 (see [5,7]), a chip with dimensions comparable to the presently used TCG-3880 (XI-200), which measures 2.50 mm × 3.33 mm on the outside. However, because it was designed for bio-chemical measurements in a flow, the interaction area – the area within the hot junctions of the thermopile – was rather large, while for the XI-200 this area is very small. When measuring minute samples (sub-milligram), a small interaction area suffices, for an enzyme–liquid interface the sensitivity is proportional to the interaction area [5,20]. These chips behaved well in the liquid flow. However, after spin coating them with the polyvinyl pyridine and the enzyme, the membranes broke, and no further experiments were carried out. In spin-coating experi-

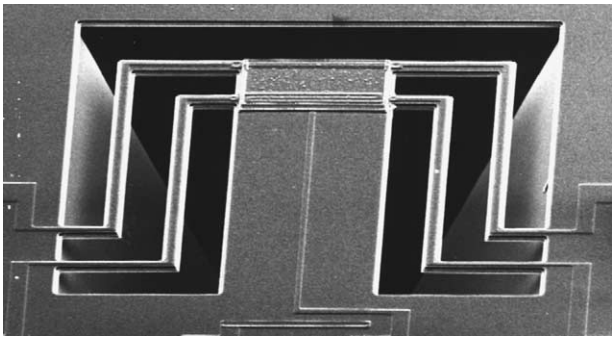

Fig. 6. Top view of a thermal properties sensor by von Arx [22] made with silicon technology, using front-side bulk etching of silicon.

ments with the XI-200, membranes did survive, although the layers were probably much thinner now.

For dry applications, the thin dielectric membranes are especially suitable. There are many dry applications, for chemical sensing [21], for measurement of the thermal and thermoelectric properties of CMOS-process layers [22,23], for materials research [24,25] and magnetic properties of thin films [26,27], and, for high-speed scanning calorimetric applications in general [28–36,39–41].

An interesting aspect of the work of Kerness is the integration of the calorimeter and CMOS amplifier electronics in one chip, made using a standard foundry CMOS process. The chip includes a chemical interface layer of PDMS (spray- or drop-coated), and has a typical resolution of about 10 ppm for such vapors as toluene or *n*-octane, with a time constant well below 1 s [21]. The electronics makes the output signal large and robust, requiring no further external amplifier electronics.

Von Arx made many structures to measure all kind of thermal and thermoelectric properties of the CMOS process layers. Where Kerness used closed membranes with bulk micro-machining of silicon from the back, von Arx used bulk micro-machining of silicon from the front, creating cantilever beams with added, narrow bridges to support electrical connections. Fig. 6 shows and example of such a device, Fig. 7 shows the layout and process used to fabricate these devices.

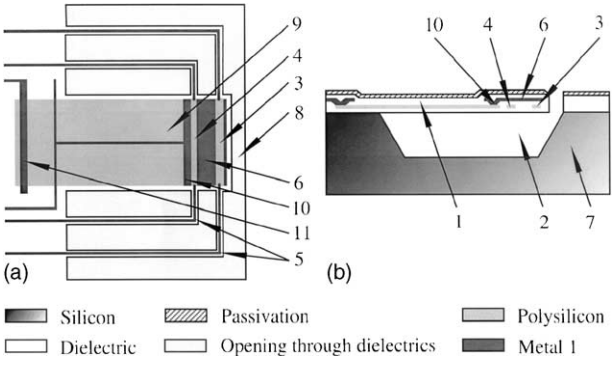

Fig. 7. Layout and process of the thermal properties sensor of Fig. 6. After the process if finished, the silicon is partially etched away (2) through the openings in the dielectrics (8).

While these devices have been made by researchers originating from the silicon sensors community, thin film calorimeter chips were also developed by researchers from the materials research community, which led to quite a different approach. Allen and Hellman both developed devices based on SiN membranes, but they used resistive heater and sensing elements, rather than polysilicon. Their objective was to minimize the addenda – the name Hellman gave to the chip's own heat capacity – in order to obtain a high-speed scanning calorimeter chip. Suddenly, scanning rates went up from K/min in standard DSC to many kK/s for these chip calorimeters.

Fig. 8 shows the typical cross-section and lay-out of the chip calorimeter developed by Allen et al. [24]. They used a metal resistive heater/temperature sensor, and by keeping the dimensions small, they have been able to attain very high heating rates of the order of 30 kK/s. As metallization, they have tried out many metals, including Ag, Al, Au, Ni and Pt. Directly on top of the metal, the sample layer to be investigated was deposited, and the ability to choose a metal means that you are able to optimize the combination of metal and sample, i.e., to have them interact maximally or not at all. In this way, Allen et al. were able to show the strong deviation of the melting points of nano-sized metal particles, compared to the bulk value.

The typical membrane lateral dimensions are 7 mm × 3 mm, the typical thickness 40–180 nm, see [25] for an extensive description of the design, theory and fabrication process.

A similar technology has been developed by Hellman and coworkers [26,27] to make calorimeter chips to investigate the thermal properties of layers. Their chips are 10 mm × 10 mm, with a 5 mm × 5 mm SiN membrane of about 180 nm thickness. They make use of Pt as metallization layer for heating and temperature sensing between 40–800 K, but also use Nb-Si semi-conductor resistances for temperature measurement at the lowest temperatures (1.5–40 K), where the Pt thermometer is not sensitive enough. They aimed at reaching a small sensor heat capacity (addenda), which is measured as about 4 μJ/K at room temperature.

The group of Paul at Freiburg University used the thin film technology to make a microDTA system, using standard IC-technology steps such as polysilicon heaters and various dielectric layers. Special is the TiW thermistor they use for temperature measurement [28].

Xensor Integration have manufactured calorimeter chips to measure the heat released when crystal damage, induced by ion implantation or nuclear radiation, is annealed away. This sensor (XI-118) has a 8.5 mm × 8.5 mm SiN membrane, 500 nm thick in a 10 mm × 10 mm frame of silicon, see Figs. 9 and 10. In the middle the sensor has a monocrystalline silicon island of about 2.5 mm × 2.5 mm and a thickness of 3 μm [7], intended to accumulate the radiation damage. Fig. 5c shows the technology for this device. Here, the heater was made of polysilicon, and the temperature sensor consisted of a polysilicon-Al thermopile. The sensors were sawn out as twins to be able to do differential scan-

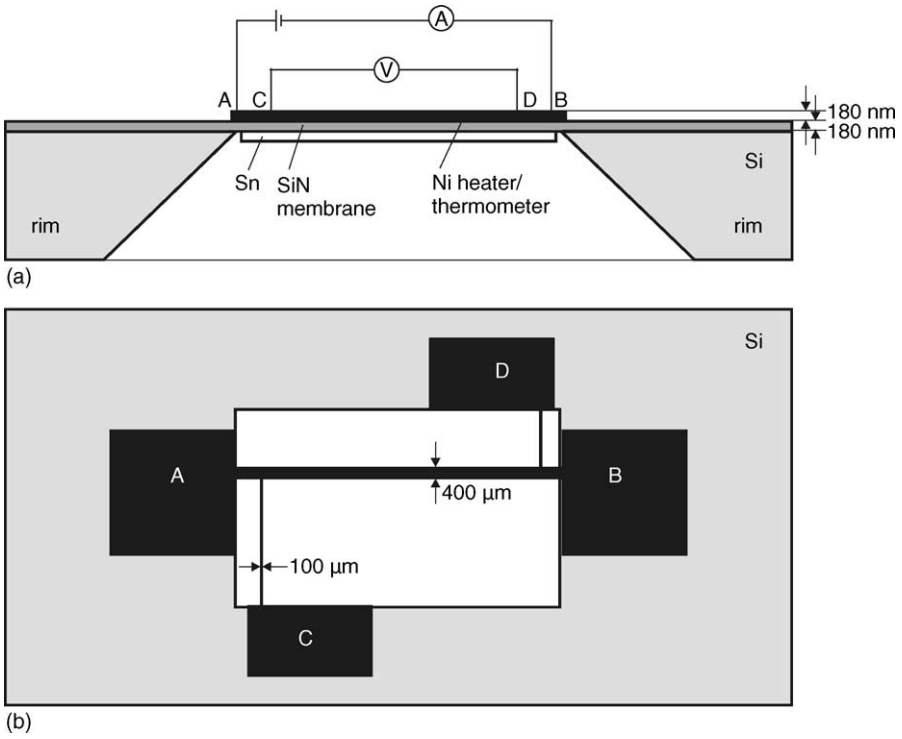

Fig. 8. Cross-section and top-view ut-away view of the membrane area of the nanocalorimeter chip used by Allen et al to study thin films. The SiN membrane thickness is typically of the order of 40–200 nm, as metallization Ag, Al, Au, Ni, Pt and other metals can be used.

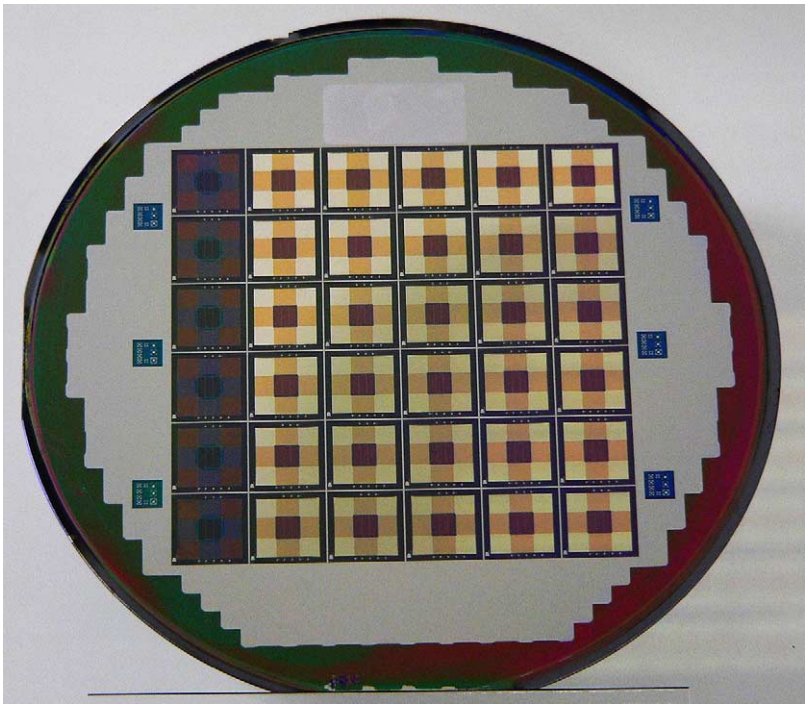

Fig. 9. Hundred-millimeter wafer with XI-118 radiation-damage calorimetric sensors measuring 10 mm × 10 mm each, with 8.5 mm × 8.5 mm SiN membranes of 500 nm thickness. The dark square in the middle of each membrane is a mono-silicon island 3 μm thick as indicated in Fig. 5b, the poly-Si/Al thermopile is seen as the four light-colored blocks, while the even lighter corner blocks are SiN membrane without further layers. In the left row devices the whole membrane is 3 μm thick mono-silicon, while the center silicon island is now 500 μm thick, just as the frame.

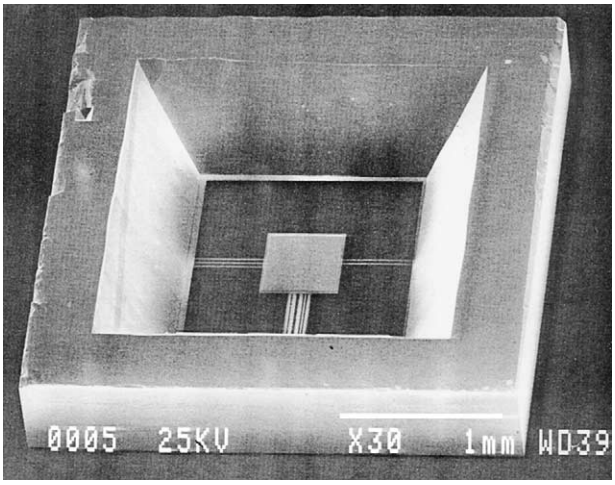

Fig. 10. Chip (similar in technology to XI-118) made in an ECE-KOH bulk-etched process to fabricate SiN membranes with mono-crystalline silicon islands of arbitrary shape underneath them [7]. SEM shows view into the cavity from the backside.

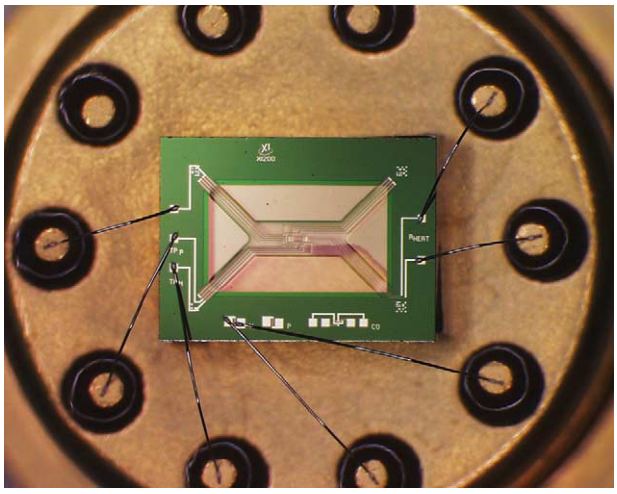

Fig. 11. XI-200 chip on a TO-5 header, forming the TCG-3880.

ning calorimetry. In contrast to the designs of Hellman and Allen, here the interaction area has been made very large. This will slow down the heating rate of the device, but it increases the total heat released by the annealing. Because of the good thermal conductivity of mono-silicon, the island will ensure a rather good temperature homogeneity between the island and the hot junctions of the thermopile.

Successful measurements were made, but not reported. At the university of Montreal, however, they not only performed but also published such measurements recently with devices resembling those of Allen [29].

Where the XI-118, designed for DSC measurements, was never operated as such, another design by Xensor, the XI-200/TCG-3880, and to some extent its predecessor, XI-120/TCG-3575 [30], have been widely used for calorimetry. These chips were designed for quite another application, the measurement of the thermal conductivity of a gas. Therefore, some features were optimized for this application, which has an adverse effect on the calorimetric performance. In particular, the heater is effectively formed by two strips of about 100 μm × 5 μm, separated 50 μm, and the thermocouple hot junctions are located some 50–100 μm away from the heater strips, see Figs. 11 and 12. This was done to avoid any polysilicon-aluminum cross-over in the design, and have ample lateral separation between heater and thermopile, to improve the life time and increase the maximum allowable voltages in the device, while making thin layers.

This leads to a much lower temperature at the hot junctions of the thermopile, compared to that of the heater, the difference can be many tens of percents. Therefore, in order to obtain proper results, extensive modeling has to be performed. Especially, the group of Schick has done a lot of work in this area [31–36]. Figs. 13 and 14 show some typical results of the group of Schick obtained with the TCG-3880 chips. These figures show, that heat capacity is not a fixed property, but depends on the experimental circumstances.

Fig. 13 shows the results on melting at different scanning rates up to 2700 K/s. The authors [36] find it gives clear evidence for the validity of a melting-recrystallization-remelting process for PET. After isothermal cold crystallization, the sample was quenched below glass transition at 30 °C. The quenching rate was 10^4 K/s. Then the measurements were performed at different scanning rates. The melting curves and the subsequent cooling curves at the same rates are shown in Fig. 14. Dramatic changes in the shape of the melting peaks appear depending on heating rate. On cooling no crystallization occurs and the glass transition of the amorphous PET is seen.

The melting curves for relatively thin (10 μm) and thick (24 μm) samples after cold crystallization are shown in Fig. 14. For the thickest sample a well pronounced shoul-

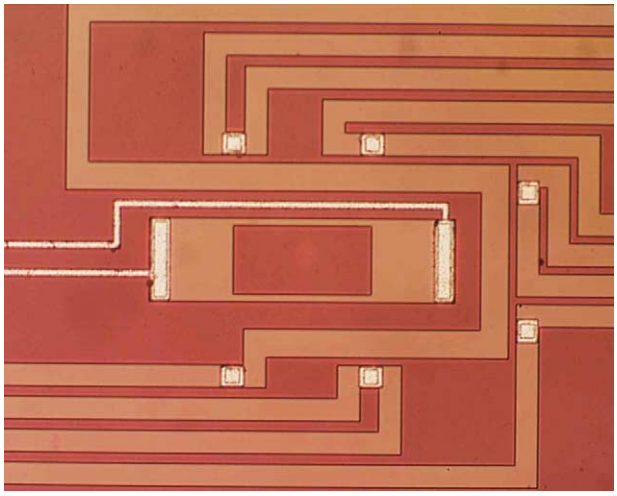

Fig. 12. Close-up of the center of the XI-200 chip, showing the central heater and the hot junctions (6× Al dot) of the p-type poly-Si vs. n-type poly-Si thermopile around it.

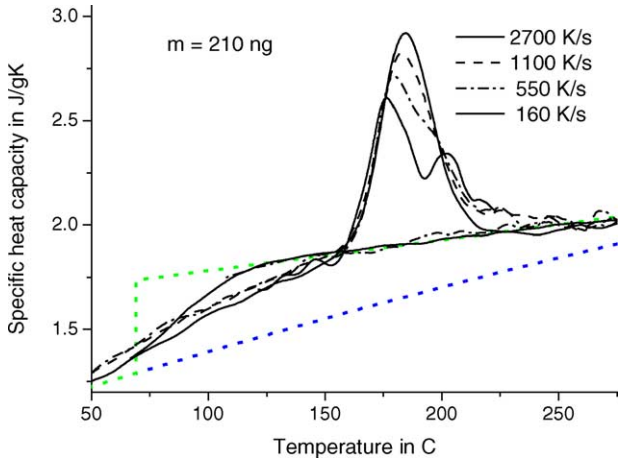

Fig. 13. Heat capacity of a 210 ng PET sample at different scanning rates, measured after fast cooling from the temperature of crystallization. The sample was crystallized at 133 °C for 1 h. The curves for completely amorphous and crystalline PET – dotted lines – are shown according to the ATHAS databank [37].

der appears above 200 °C, while for the thinnest sample basically nothing is seen at such temperatures. From trans-crystallinity studies it is known that layers of such thickness ca. 10 μm are influenced by trans-crystallinity [38]. Here, the authors conclude that this means that the morphology in the thinner samples is more stable compared to the thicker sample.

Merzlyakov proposes to evade the problem of the heater-thermopile gap and the related time and temperature lag in the TCG-3880 chip calorimeter by using the heating resistor not only for heating, but also to measure the temperature, just as Allen and Hellman do [39]. In this way, he envisions to reach heating and cooling rates up to 300 kK/s.

The thermopile of these devices functions properly and with good sensitivity between 20 K and 600 K. Below 20 K, the sensitivity drops, but the device is still capable of measurement. Above 600 K, the melting temperature of the aluminum interconnection is approached, and in combination with electrical currents through the aluminum leads, the risk of destroying the device rapidly increases with temperatures towards 800 K.

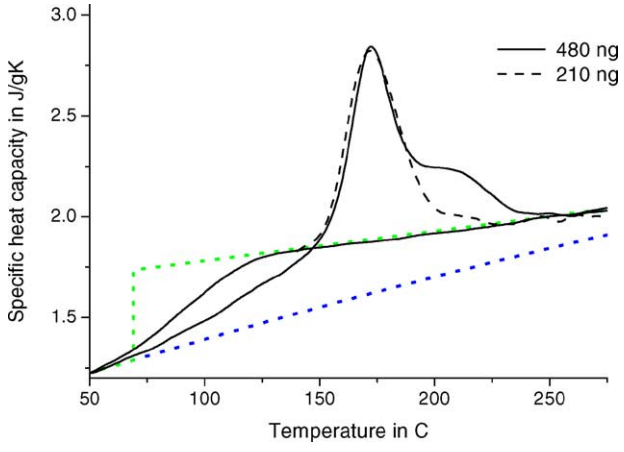

Fig. 14. Heat capacity of two PET samples: 480 ng (ca. 24 μm thick) – solid line and 210 ng (10 μm) – dashed line at the scanning rate 2700 K/s after fast cooling from the temperature of crystallization. The samples were crystallized at 114 °C for 10 h. The dotted lines are again from the ATHAS databank [37].

Using AC-calorimetry, Minakov etal were able to perform measurements from 10–300 K in magnetic fields up to 8 T with the TCG-3880 [40].

Also industry is becoming interested in calorimeter chips, especially for its application towards polymer research, as indicated by the work of the group of Mathot at DSM, the Netherlands [41].

3.2. Figure of Merit

For high-speed DSC, the field of measuring material properties at high scanning rates, a different FoM will apply than for chemical calorimeters. Here, it is not so much the area as the scan rate in which we are interested, since higher scan rates allow us to observe phenomena that take place when materials are heated or cooled in a range of (high) scan rates unavailable with traditional DSC instruments. We will name this FoM the $\mathrm{FoM}_{\mathrm{scan}}$, as it focuses on scan rate.

Here, it is of interest to compare the signal-to-noise ratio SNR at the maximum scan rate, and the maximum scan rate itself. Since heating can be done at any rate, we will compare cooling scan rates, which are inversely proportional to the thermal *RC* time constant of the chip plus the sample. You may also assume that the electrical noise will be filtered with the same time constant, since there is little sense in incorporating electrical noise from a frequency band not incorporating thermal signals.

Now, we let us define our FoM as the product of signal-to-noise ratio at maximum scan rate and the maximum scan rate itself. The output signal is proportional to the scan rate in K/s. This is equal to the maximum temperature difference $\Delta T_{\max}$ of the device (the maximum attainable temperature increase with respect to the base temperature) divided by the *RC* time constant. And the output signal is also proportional to the heat capacitance of the sample, which is C_{s}, where C_{s} is the heat capacitance of the sample for cooling, or for a phase change or whatever. If we assume that the noise of the chip is independent of frequency (white noise), the noise voltage u_{n} is then inversely proportional to the square root of the thermal *RC* time constant, also used for filtering the electrical signal. Now we arrive at the following expression for the FoM, the product of scan rate and SNR:

$$\mathrm{FoM}_{\mathrm{scan}} \rightarrow \frac{\Delta T_{\max}}{RC} \times \frac{C_{\mathrm{s}}\,\Delta T_{\max} S}{RC u_{\mathrm{n}}} = \frac{C_{\mathrm{s}}\,\Delta T_{\max}^2 S}{[R(C_{\mathrm{s}} + C_{\mathrm{a}})]^{1.5} u_{\mathrm{n,1Hz}}} \quad (2)$$

In this expression, the thermal capacitance C has been specified as the sum of the sample heat capacitance C_s, and the chip heat capacitance C_a, the addenda as Hellman calls it. The noise u_n has been represented by the noise voltage of the chip in the 0–1 Hz band $u_{n,1Hz}$ times the square root of the electric filtering band width $1/(RC)^{0.5}$, assuming white (is frequency-independent) noise.

Note, that the maximum scan rate appears twice in this FoM, since not only is its high value a bonus for phenomenological reasons, but it will also lead to a larger signal.

It can be seen that this FoM has a maximum for $C_s = 2C_a$. This maximum is larger, when C_a is smaller. Then, the FoM becomes:

$$\mathrm{FoM}_{\mathrm{scan}} = \frac{\Delta T_{\max}^2 S_{\mathrm{TP}}}{(RC_a)^{0.5} u_{n,1Hz}} \tag{3}$$

where S_{TP} is the sensitivity of the temperature sensing element, here taken as a thermopile in V/K, and where $S = RS_{TP}$. It can be derived from the above expressions, that a large sample mass and high thermal resistance in itself leads to a better SNR. However, larger R and C will lower the maximum scan rate and prevent phenomena at higher scan rates to be observed.

4. Discussion

As already remarked by many authors, chips can be used for high-speed DSC to obtain very high rates of heating and cooling. Compared to the 10 K/s that is now obtainable with HperDSC™ (Perkin-Elmer) and similar DSC instruments, the 1 MK/s heating and cooling rates that chip calorimeters can reach is five orders of magnitude faster. This is the difference between not being able to capture what is actually happening in, especially, polymer technology, and being able to see all effects at different, realistic, time scales.

With different calorimetric applications, different chip designs and technologies are required. For liquid applications involving enzymatically promoted reactions, chips with large interaction areas and relatively thick and therefore strong membranes are the proper choice. For analyzing thermo-physical phenomena where high-speed scanning is required, such as cooling of polymers or transition effects in materials, the membranes do not need to be strong, since the samples are small to allow ultra-high-speed scanning. There, a thin membrane adding little heat capacitance is preferred.

The overview above shows that many universities have developed, with good success, their own calorimeter chips, and also many universities have with benefit used calorimetric chips available commercially. The number of applications for these chip calorimeters is already large, reflecting the versatility of the calorimetric measurement field.

References

[1] B. Wunderlich, Fast and Super-fast DTA and Calorimetry, in: Proceedings-CD of the 32nd Conference on NATAS, Williamsburg, VA, USA, 4–6 October 2004, pdf-018.
[2] P. Bataillard, E. Steffgen, S. Maemmerli, A. Manz, H.M. Widmer, An integrated silicon thermopile as biosensor for the thermal monitoring of glucose, urea and penicillin, Biosens. Bioelectron. 8 (1993) 89–98.
[3] www.xensor.nl.
[4] P. Bataillard, Calorimetric sensing in bio-analytical chemistry: principles, applications and trends, Trends Anal. Chem. 12 (1993) 387–394.
[5] A.W. van Herwaarden, P.M. Sarro, J.W. Gardner, P. Bataillard, Liquid and gas micro-calorimeters for (bio)chemical measurements, Sens. Actuators A43 (1994) 24–30.
[6] www.vivactis.com.
[7] P.M. Sarro, A.W. van Herwaarden, W. van der Vlist, A silicon–silicon nitride membrane fabrication process fro smart thermal sensors, Sens. Actuators A41–42 (1994) 666–671.
[8] W. Winter, G.W.H. Höhne, Chip-calorimeter for small samples, Thermochim. Acta 403 (2003) 43–53.
[9] J. Lerchner, J. Seidel, G. Wolf, E. Weber, Calorimetric detection of organic vapours using inclusion reactions with organic coating materials, Sens. Actuators, B 32 (1996) 71–75.
[10] J. Lerchner, R. Oehmgen, G. Wolf, P. Le Parlour, J.-L. Daudon, Supermicrocalorimetric devices for the investigation of small samples, High Temperatures-High Pressures 30 (1998) 701–708.
[11] J. Lerchner, A. Wolf, G. Wolf, Recent developments in integrated circuit calorimetry, J. Thermal Anal. Calorimetry 57 (1999) 241–251.
[12] D. Caspary, M. Schröpfer, J. Lerchner, G. Wolf, A high resolution IC-calorimeter for the determination of heats of absorption onto thin coatings, Thermochim. Acta 337 (1999) 19–26.
[13] J. Lerchner, D. Caspary, G. Wolf, Calorimetric detection of volatile organic compounds, Sens. Actuators, B 70 (2000) 57–66.
[14] J. Lerchner, G. Wolf, C. Auguet, V. Torra, Accuracy in integrated circuit (IC) calorimeters, Thermochim. Acta 382 (2002) 65–76.
[15] Y.S. Liu, V.M. Ugaz, W.J. Rogers, M.S. Mannan, S.R. Saraf, Development of a nanocalorimeter for material characterization, in: Proceedings-CD of the 32nd Conference on NATAS, Williamsburg, VA, USA, 4–6 October 2004, pdf-111.
[16] V. Torra, C. Auguet, J. Lerchner, P. Marinelli, H. Tachoire, Identification of micro-scale calorimetric devices. I. Establishing the experimental rules for accurate measurements, J. Thermal Anal. Calorimetry 66 (2001) 255–264.
[17] C. Auguet, F. Martorell, F. Moll, V. Torra, Identification of micro-scale calorimetric devices. II. Heat transfer models from two or three-dimensional analysis, J. Thermal Anal. Calorimetry 70 (2002) 277.
[18] C. Auguet, J. Lerchner, V. Torra, G. Wolf, Identification of micro-scale calorimetric devices III: the 3-D effects, J. Thermal Anal. Calorimetry 71 (2003) 407–419.
[19] C. Auguet, J. Lerchner, V. Torra, G. Wolf, Identification of micro-scale calorimetric devices. IV. Descriptive models in 3-D, J. Thermal Anal. Calorimetry 71 (2003) 951–966.
[20] A.W. van Herwaarden, Physical principles of thermal sensors, Sens. Mater. 8 (1996) 373–387.
[21] N. Kerness, A. Koll, A. Schaufelbühl, C. Hagleitner, A. Hierlemann, O. Brand, H. Baltes, "N-Well based CMOS Calorimetric Chemical Sensors", in: Proceedings of MEMS 2000, pp. 96–101.
[22] M. von Arx, Thermal properties of CMOS thin films, Ph.D. thesis, ETH 12743, 1998, Swiss Federal Institute of Technology, Zurich.
[23] M. von Arx, O. Paul, H. Baltes, Test structures to measure the heat capacity of CMOS layer structures, IEEE Tr, Semicond. Manufact. 11 (1998) 217–224.
[24] S.L. Lai, G. Ramanath, L.H. Allen, P. Infante, Z. Mai, High-speed (10^4 °C/s) scanning microcalorimetr with monolayer sensitivity (J/m^2), Appl. Phys. Lett. 67 (1995) 1229–1231.

[25] E.A. Olsen, M.Y. Efremov, M. Zhang, Z. Zhang, L.H. Allen, J. MEMS 12 (2003) 355–364.
[26] D.W. Denlinger, E.N. Abarra, K. Allen, P.W. Rooney, M.T. Messer, S.K. Watson, F. Hellman, Thin film microcalorimeter for heat capacity measurements from 1.5 to 800 K, Rev. Sci. Instrum. 65 (1994) 946–959.
[27] B.L. Zink, B. Revaz, R. Sappey, F. Hellman, Thin film microcalorimeter for heat capacity measurements in high magnetic fields, Rev. Sci. Instrum. 73 (2002) 1841–1884.
[28] P. Ruther, M. Herrscher, O. Paul, A micro differential thermal analysis (μDTA) system, in: Proceedings of the 17th IEEE Conference on MEMS, Maastricht, Jan 2004, pp. 165–168.
[29] R. Karmouch, J.-F. Mercure, F. Schietekatte, Nanocalorimeter fabrication procedure and data analysis for investigations on implantation damage annealing, Thermochim. Acta, doi:10.1016/j.tca.2004.12.014.
[30] M. Merzliakov, Integrated circuit thermopile as a new type of temperature modulated calorimeter, Thermochim. Acta 403 (2003) 65–81.
[31] S.A. Adamovsky, A.A. Minakov, C. Schick, Scanning microcalorimetry at high cooling rate, Thermochim. Acta 403 (2003) 55–63.
[32] M. Merzlyakov, C. Schick, IC thermopile as a new type of temperature modulated calorimeter, NATAS Notes 34 (4) (2003) 18–21.
[33] A.A. Minakov, S.A. Adamovsky, C. Schick, Ultra fast calorimetry on controlled cooling and heating up to 10,000 K/s and isothermally with millisecond time resolution (Poster), e-Polymers 2003, available on the web site: http://www.polymers.tudelft.nl/wubweb/Schick-abstract.htm.
[34] A.A. Minakov, D.A. Mordvintsev, C. Schick, Reorganization of polymer crystals studied by fast scanning calorimetry, Faraday Discuss. 128 (2005) 261–270.
[35] For a complete overview of the work of the group of Prof. Schick, see the web site: www.uni-rostock.de/fakult/manafak/physik/poly/polymerphysics.htm.
[36] A.A. Minakov, D.A. Mordvintsev, C. Schick, Polymer 45 (11) (2004) 3755–3763.
[37] B. Wunderlich, et al., see on WWW URL: http://web.utk.edu/~athas/databank/intro.html.
[38] K.H. Nitta, Y. Yamamoto, e-Polymers 24 (2003) 1–11.
[39] M. Merzlyakov, Method of rapid (10,000 K/s) controlled cooling and heating of thin samples, in: Proceedings-CD of the 32nd Conference on NATAS, Williamsburg, VA, USA, 4–6 October 2004, pdf-027.
[40] A.A. Minakov, S.B. Roy, Y.V. Bugoslavsky, L.F. Cohen, Thin-film alternating current nanocalorimeter for low temperatures and high magnetic fields, Rev. Sci. Instrum. 76 (2005) art no. 043906.
[41] T. Pijpers, G. V. Poel, R. Tol, C. Schick, V. Mathot, Metastability in polymer systems studied at extreme conditions, including low to very high scanning rates, in: Proceedings-CD of the 32nd Conference on NATAS, Williamsburg, VA, USA, 4–6 October 2004, pdf-019;
T.F.J. Pijpers, V.B.F. Mathot, B. Goderis, R.L. Scherrenberg, E.W. van der Vegte, High-speed calorimetry for the study of the kinetics of (de)vitrification, crystallization, and melting of macromolecules, Macromolecules 35 (9) (2002) 3601.